STATE OF KNOWLEDGE OF EUROPA

**TAKEN FROM THE REPORT OF THE
EUROPA ORBITER SCIENCE DEFINITION TEAM**

June 1999

STATE OF KNOWLEDGE OF EUROPA

TABLE OF CONTENTS

TABLE OF TABLES

TABLE OF FIGURES

STATE OF KNOWLEDGE OF EUROPA

Taken from the Report of the
Europa Orbiter Science Definition Team

This description of the state of knowledge Europa and the outstanding scientific questions was developed in conjunction with the Europa Orbiter Science Definition Team (SDT).* In the event of conflict between the Science Definition Team Report description of the Europa Orbiter mission and the AO, the AO takes precedence. The basic parameters of the reference mission and the Europa Orbiter "strawman payload" were developed by the Europa Orbiter Science Definition Team.

1.   Physical Properties

1.1   Size, Mass, and Density

Europa, the smallest of the four Galilean satellites of Jupiter, is about the size of the Earth's Moon. Its density of 3 gm/cm^3 indicates that it is primarily a silicate/iron body, as distinguished from the ice/rock/iron compositions inferred for the low-density satellites, Ganymede and Callisto (1.94 and 1.85 gm/cm^3). However, it is significantly less dense than its neighbor, Io, the innermost of the Galilean moons (~3.54 gm/cm^3) or even the iron-poor Moon (3.3 gm/cm^3), implying some lower density component in its bulk composition, presumably water in some form. If the water is incorporated in low-density hydrated silicates, only a thin surface coating of water ice is implied (<few km). On the other hand, if the bulk of the satellite is similar to Io, a layer of ~100 km of ice is required to achieve the observed bulk density (Schubert *et al.*, 1986; Cassen *et al.*, 1982). Current evidence favors the latter interpretation (see below).

1.2   Internal Structure

Tracking data from the Galileo mission has been used to measure the higher order terms in Europa's gravity field, specifically the 2nd degree, 0th order J_2 and the 2nd degree and order C_{22} coefficients. These deviations from a spherically symmetric field arise from Europa's spin and tidal distortion from Jupiter, and their magnitude is related to the satellite's interior structure. Under the assumption of overall hydrostatic equilibrium within the satellite (testable by consistency between determinations from several flybys), the J_2 and C_{22} coefficients can be used to calculate the axial moment of inertia, C/MR^2. The value of this moment is in turn related directly to the degree that mass is concentrated toward the center of the body, with a homogeneous body having a moment of inertia of exactly 0.40. The current best value of C/MR^2 from Galileo analysis is 0.346 ± 0.005 (Anderson *et al.*, 1998). This suggests a significant degree of internal differentiation, concentrating mass toward the center. Multi-layer models can be constructed which match this moment of inertia and the bulk density by varying the assumed densities of the layers. Assuming that the high-density layers are rock and iron or iron sulfide in some mixture, the resultant models require 80-170 km of material with density ~1, appropriate for either ice or liquid water. Taking Io as a model for the properties of the non-water bulk of Europa's makeup, these authors' preferred interior structure model is three layers consisting of an iron/iron sulfide core, a rocky mantle and a ice/water crust ~100-150 km thick.

1.3   Orbital Properties, Tides

All the Galilean satellites have nearly circular orbits in the plane of Jupiter's equator, with Europa having a mean distance of about 9.5 Jupiter radii from the primary planet (1 R_J = 71,429 km). A single satellite in such an orbit would be expected to establish a perfectly circular, synchronous (same side facing the primary) orbit due to tidal interactions. However, the inner three large satellites, Io, Europa, and Ganymede participate in what is called a Laplace resonance, where their orbital periods are locked to each other. This results in a resonant forcing of the satellites' orbital elements, particularly eccentricity. Even slightly eccentric orbits potentially have major effects on the satellites. The large body tides raised by Jupiter on the satellites vary in amplitude and phase as the satellite goes around the planet in an eccentric orbit. A varying tide can produce substantial heating in the interior of the satellites, depending on the distance to Jupiter (the size of the time varying tide is proportional to $1/a^3$) and how well tidal energy is dissipated in the body of the satellite (the "Q" of the body). Peale *et al.* (1979), in a seminal paper predicting volcanism on Io, first pointed out this method of producing significant tidal heating in the system.

Table 1: Europa encounter geometry and gravity results

	E4	E6	E11	E12
Latitude (°)	-1.7	-17.0	25.7	-98.7
Longitude (°)	36.8	324.7	140.6	225.0
Altitude (km)	697	591	2048	205
SEP (°)	24.6	25.2	89.0	54.6
Direction Cosines for line of sight				
Cross-track	0.772	0.656	-0.744	0.985
Along-track	0.634	0.729	0.569	0.068
Normal	-0.035	-0.194	0.350	-0.160
Coherent Doppler?	No	No	Yes	Yes
J_2 $(\times 10^{-6})$	215 ± 102	438 ± 45	442 ± 28	438 ± 9
C_{22} $(\times 10^{-6})$	65 ± 31	132 ± 13	133 ± 8	132 ± 2
μ	0.999	0.995	0.986	0.847
C/MR²	0.264 ± 0.041	0.347 ± 0.014	0.349 ± 0.009	0.348 ± 0.002

J.D. Anderson, G. Schubert, R. A. Jacobson, E.L. Lau, W.B. Moore, W.L. Sjogren. "Europa's Differentiated Internal Structure: Inferences from Four Galileo Encounters." Science, Vol. 281, 25 September 1998, p.2019

Table 2: Galilean Satellite Orbital Data

	Satellite	a $(10^3$ km)	Orbital Period (days)	Rot. Period (days)	e	I (deg)
I	Io	421.6	1.769138	S	0.041	0.040
II	Europa	670.9	3.551810	S	0.0101	0.470
III	Ganymede	1,070	7.154553	S	0.0015	0.195
IV	Callisto	1,833	16.689018	S	0.007	0.281

Charles F. Yoder. "Astrometric and Geodetic Properties of Earth and the Solar System," Global Earth Physics: A Handbook Of Physical Constants, 1995. p.19.

Table 3: Galilean Satellite Physical Properties

Satellite	Radius (km)	Mass $(10^{20}$ kg)	Density (gm cm⁻³)	Geom. albedo
JI Io	1821.3 ± 0.2	893.3 ± 1.5	3.530 ± 0.006	0.61
JII Europa	1565 ± 8	479.7 ± 1.5	2.99 ± 0.05	0.64
JIII Ganymede	2634 ± 10	1482 ± 1	1.94 ± 0.02	0.42
JIV Callisto	2403 ± 5	1076 ± 1	1.851 ± 0.004	0.20

Charles F. Yoder. "Astrometric and Geodetic Properties of Earth and the Solar System," Global Earth Physics: A Handbook Of Physical Constants, 1995. P.17.

Tidal heating of the Galilean satellites is key to understanding their history and geology. Io's unprecedented level of volcanism results from tidal heating, and Ganymede's differentiated structure and even the existence of its internal magnetic field may well be results of its history of tidal heating (Anderson *et al.*, 1996; Showman et al., 1997). One of the principle reasons for believing that Europa may have a liquid ocean is that theoretical calculations suggest that tidal heating may be sufficient to keep such an ocean from freezing solid (Cassen *et al.*, 1979; Cassen *et al.*, 1980; Squyres *et al.*, 1983; Ojkangas and Stevenson, 1989). The amount of tidal heat generation compared with radiogenic heat depends strongly on the geophysical and rheological parameters assumed. Table 4 (after Shubert *et al.*, 1986) lists the major sources of heat for the Galilean satellites. Estimates of tidal heating for Europa range from the table value of 0.7×10^{11} W (for a solid body, from Cassen *et al.*, 1982) to more than 20 times that, 1.6×10^{12} W for a ice/ocean/silicate mantle model (Squyres *et al.*, 1983).

Table 4:   Comparison of heating from various sources for planetary satellites

Satellite	Total Accretional Energy per Unit Mass (MJ kg^{-1})	Total Accretional Energy (10^{27} J)	$\Delta T = E\,\mathrm{acc}/c^{b}$ (K)	Energy of Differentiation in % of E_{acc}	Radiogenic Heat Production Rate ^{c} (10^{11} W)	Homogeneous Tidal Heating Rate ^{d} (10^{11} W)
Moon	1.69	124	1400		6.79	
Io	1.97	176	1600	6	4.87	17
Europa	1.24	60.5	1000	5	2.50-2.66	0.7
Ganymede	2.27	338	1300	12	4.72-5.93	
Callisto	1.79	193	1000	13	3.05-3.87	
Mimas	9.29×10^{-3}	4.23×10^{-4}	5		$(1.17\text{-}1.37) \times 10^{-3}$	
Enceladus	1.19×10^{-2}	8.77×10^{-4}	15		$(0.89\text{-}1.05) \times 10^{-3}$	6.2×10^{-4}
Tethys	5.70×10^{-2}	4.31×10^{-2}	40		$(1.19\text{-}1.44) \times 10^{-2}$	
Dione	7.52×10^{-2}	7.91×10^{-2}	50		$(2.64\text{-}3.10) \times 10^{-2}$	
Rhea	0.130	0.325	110		$(5.30\text{-}6.25) \times 10^{-2}$	
Titan	2.09	282	1200	12	4.04-5.14	
Iapetus	0.103	0.194	130		$(2.46\text{-}2.87) \times 10^{-2}$	

[a]   Homogeneous accretion is assumed

[b]   Assumes specific heat $c = 1.2$ kJ kg^{-1} K^{-1} for the Moon, Io, and Europa; $c = 1.8$ kJ kg^{-1} K^{-1} for Ganymede, Callisto, Titan, and Mimas; $c = 1.5$ kJ kg^{-1} K^{-1} for Tethys and Dione; $c = 1.2$ kJ kg^{-1} K^{-1} for Rhea; $c = 0.8$ kJ kg^{-1} K^{-1} for Iapetus and Enceladus.

[c]   The lunar heating rate is 9.2×10^{-12} W kg^{-1}, and the chondritic heating rate is 5.45×10^{-12} W kg^{-1}. The ranges of values for the icy satellites correspond to ranges of silicate mass fractions.

[d]   Estimate for tidal heating in a completely solid satellite for Io and Europa by Cassen et al. (1982) and for Enceladus by Squyres et al. (1983).

4

Tides may also play a key role in being able to determine if a subsurface ocean is present at the current epoch. The change in tides during a Europa diurnal cycle (~3.5 days) will depend on the rigidity and structure of the crust and subsurface materials (see discussion in Sec. 2.1 of the Europa Orbiter Mission and Project Description document in the Outer Planets Program Library, which can be accessed over the Internet through URL http://outerplanets.LaRC.NASA.gov/outerplanets). The tides expected for various cases can be described by the h_2 and k_2 Love numbers. Figure 1 shows the h_2 and k_2 values associated with several possible ocean models calculated by Dr. Charles Yoder of JPL.
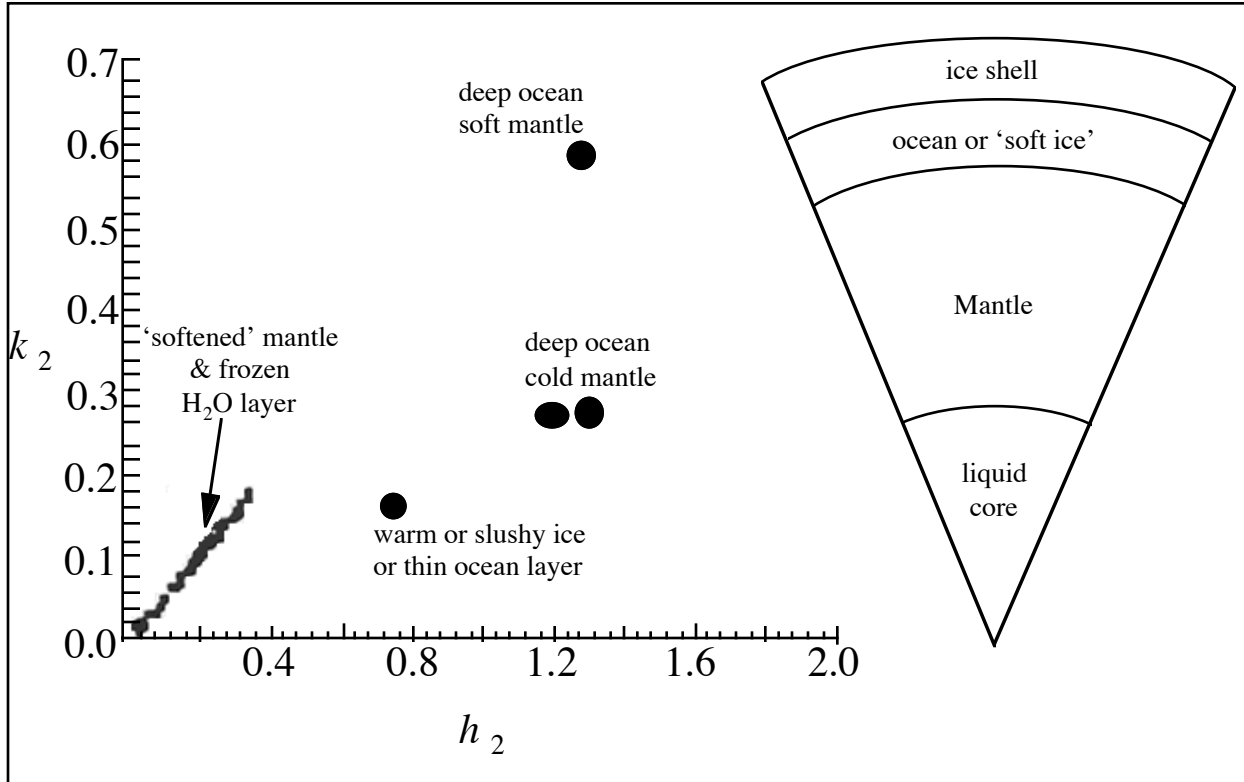

Figure 1:   Love numbers h_2 versus k_2 for a variety of structure models. The ratio $h_2/k_2 \sim 2$ for the 'frozen ocean' case while $h_2/k_2 \sim 4$ for a deep ocean.

1.4   Spectral Albedo

Europa's surface is very reflective at visible wavelengths, but absorbs light in the near infrared. These characteristics, evident even in the relatively crude photometric measurements of the 1950's, were interpreted as evidence for an ice covered surface (Kuiper, 1957; Moroz, 1965). High quality infrared spectroscopy a decade later convincingly identified the diagnostic absorptions of solid H_2O in Europa's 1-2.5 µm spectrum and demonstrated that water ice and/or frost covers a large fraction of Europa's surface (Pilcher *et al.*, 1972). Europa's visual color is "yellow-brown" resulting from some blue and ultraviolet absorbing material. In

addition, the "trailing" hemisphere (with respect to orbital motion) has ultraviolet absorptions interpreted as arising from the implantation of sulfur ions from the overtaking Jovian plasma (see Sill and Clark, 1982; Malin and Pieri, 1986 for reviews of various suggested interpretations of the source of these absorption).

Based on extensive telescopic observations and analysis of photometry from the Voyager cameras, we have a good understanding of the satellite's global and regional photometric properties. At a hemispheric scale, Europa reflects about 60% of the total solar radiation it receives (the Bond albedo). Regionally, normal reflectance (compared with a flat, diffusing white plate) ranges from 20% in the blue to 80% in the $0.6 - 1.0$ µm spectral region (Johnson *et al.*, 1983; Buratti and Golombek, 1985).

Table 5:   Summary of Photometric Properties of Europa [a]

	Voyager (Clear Filter)	Earth-based (V Filter)
Phase coefficient, ß (mag/deg)	0.0129 ± 0.0003	0.013 ± 0.001 [b]
Geometric albedo, p	$0.72 \pm$ (L) 0.62 ± 0.02 (T)	0.74 ± 0.03 (L) [c] 0.60 ± 0.03 (T)
Phase integral, q	1.09 ± 0.11	1.0 ± 0.1 [d]
Average normal reflectance, r_n (*Voyager*)	0.71 all bright plains 0.60 darker mottled terrain ($33^o < ø < 124^o$) [e] 0.48 darker mottled terrain ($ø \sim 340^o$)	
Bond albedo, A_B	0.62 ± 0.14	0.58 ± 0.14 [d]

[a] Table from Buratti (1983)

[b] Average of leading (L) and trailing (T) hemisphere values (Millis and Thompson, 1975).

[c] From Millis and Thompson (1975)

[d] Radiometric value from Morrison (1977).
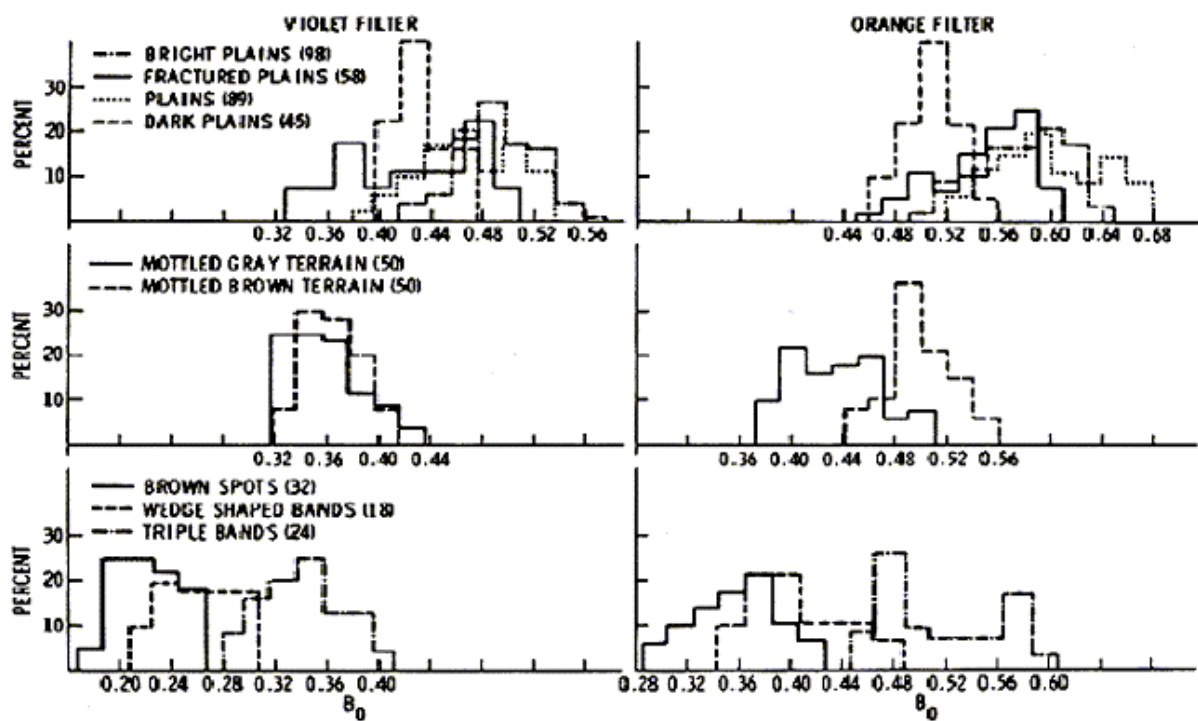
[e] ø = subspacecraft longitude.

Figure 2. Histograms of data groupings for Voyager violet and orange filters for nine Europan terrain types (figure from Buratti and Golombek 1985.)
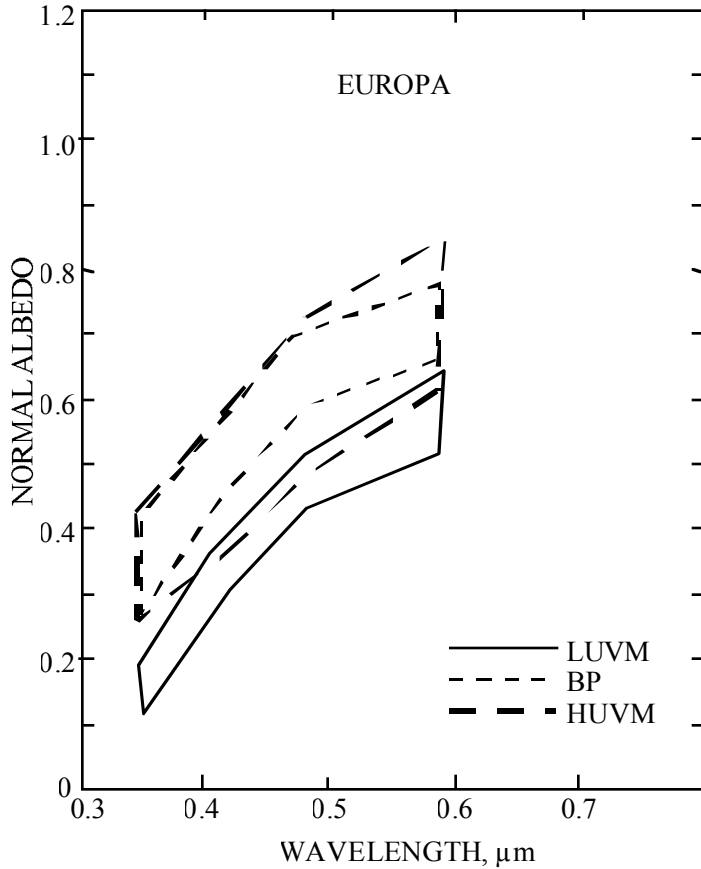
Figure 3.   Normal albedo for three different terrains on Europa (LUVM: low-ultraviolet materials; HUVM: high-ultraviolet materials; and BP: bright plains materials) shown as a function of wavelength (figure from T.V. Johnson et al. 1983).

Figure 3 shows the normal albedo spectrum as derived from Voyager imaging data. More recent results from Galileo provide albedo measurements out to 1 μm and have allowed a better determination of Europa's opposition effect, which causes the normal albedo values to be increased over the values extrapolated from Voyager data. Figure 4 shows the Galileo-based normal albedo spectra for a range of Europan terrains (Clark, et al., 1998). Figure 5 compares the surface reflectance at 5° phase to that at 0° (incident and emission angles = 35° in both cases; Helfenstein, et al., 1998) for several terrain types. Figure 6 shows the observed relationship between surface reflectance at opposition to that at 5° phase (Helfenstein, et al., 1998).
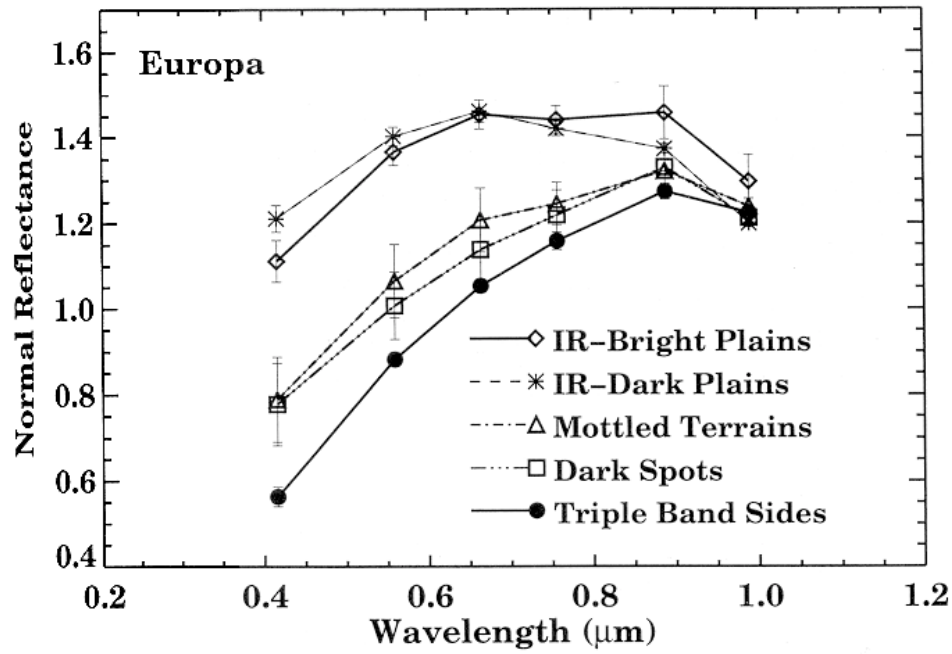
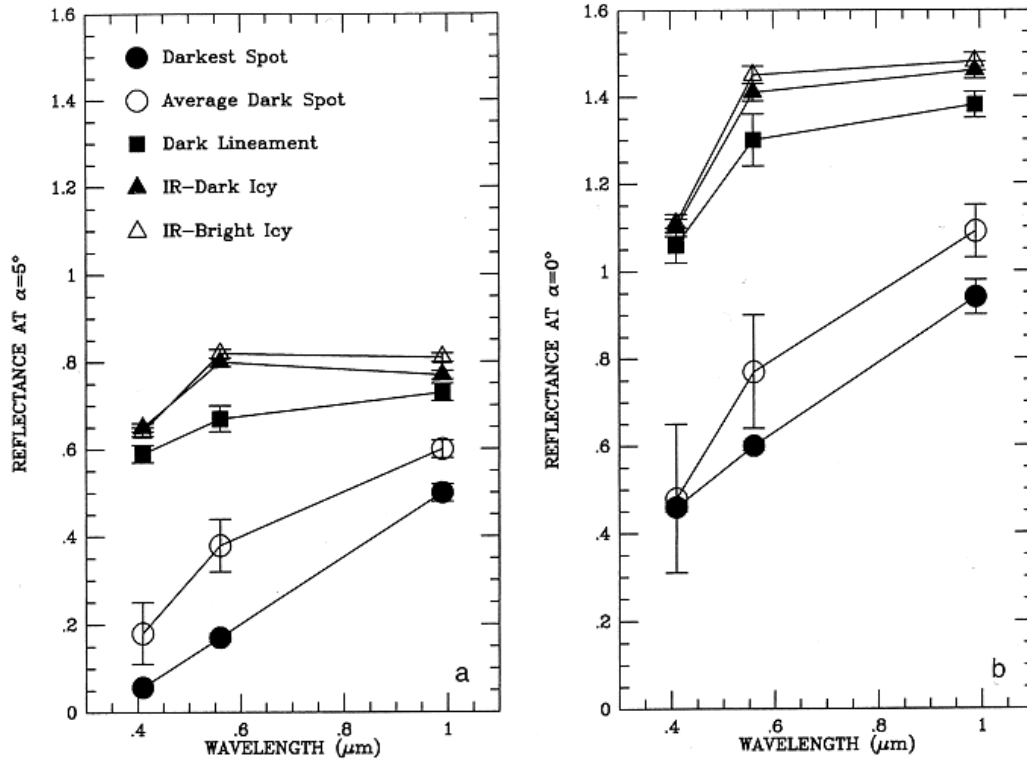**Figure 4.** Multispectral behavior of Europan terrains (from Clark, et al., 1998)

Figure 5. Absolute spectra of major Europan terrain units interpolated to i = e = 35° for (a) phase = 5°, (b) phase = 0° (from Helfenstein, et al., 1998)
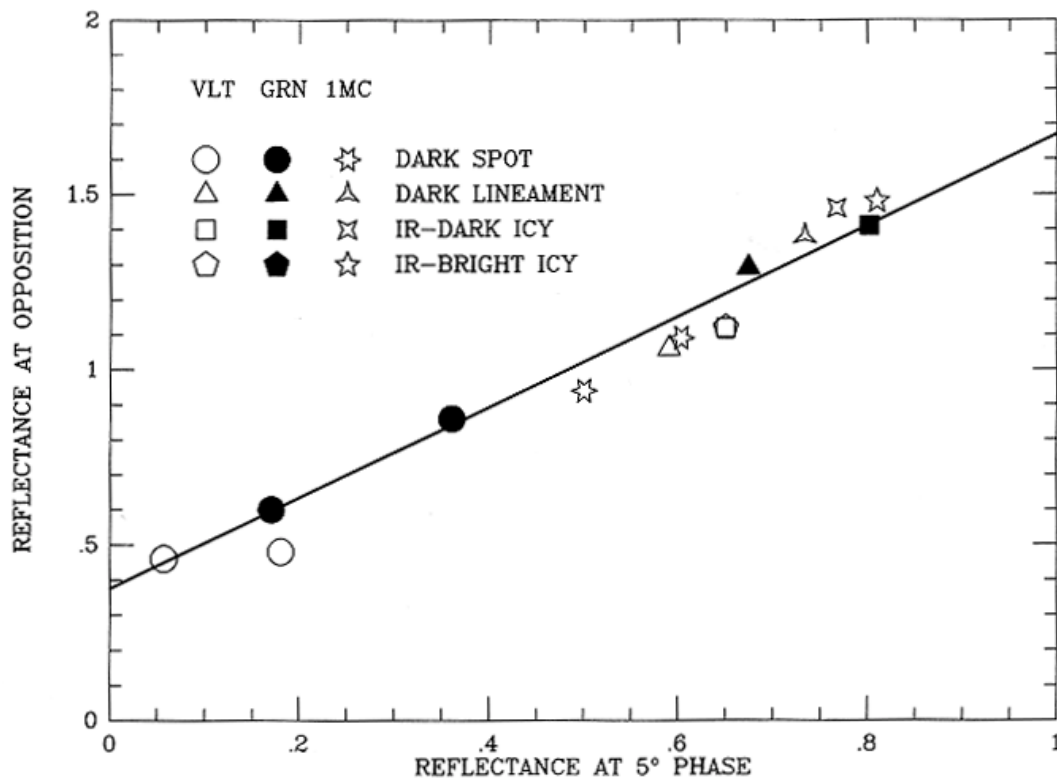
Figure 6. Extrapolated opposition albedos of Europan terrains as a function of their corresponding average reflectance at 5° phase angle (from Helfenstein, et al., 1998)

1.5   Temperature

Given Europa's high albedo, surface temperatures are expected to be very low. Morrison (1977) estimated a maximum temperature of 139 K based on photometric parameters available at the time. Telescopic brightness temperatures from sources referenced in Morrison range from 121 K (at 21 μm) to 134 K (at 8 μm). Analysis of Voyager infrared data (IRIS) by Spencer (1987) shows spatially resolved temperatures from 110 K in the late afternoon to ~85 K at night. Preliminary Galileo Photo Polarimeter/Radiometer (PPR) results at 37 μm yield a sub-solar brightness temperature of 128 K (Orton *et al.*, 1996). Ojakangas and Stevenson (1989) calculate a globally averaged temperature of ~100 K, with temperatures dropping to ~50 K at the poles.

A complete thermophysical description of Europa's surface is not available. Estimates of the thermal inertia of the surface come from modeling telescopic eclipse observations and from the Galileo PPR and Voyager IRIS data. Telescopic eclipse data at 10 μm yields a value of $1.4 \pm 0.4 \times 10^4$ ergs $cm^{-2}s^{-1/2}K^{-1}$ (Hansen, 1973). Estimates based on modeling the Voyager IRIS data range from ~3 to ~7 x 10^4 in the same units (Urquhart and Jakosky, 1996). Comparing the preliminary PPR sub-solar temperature with the Voyager nighttime value Orton *et al.* estimate

2.6 x 10^4. A complication in modeling the temperature response of icy surfaces such as Europa's is the possible effect of sunlight light penetrating, and heating, to significant depth in a transparent medium (the "solid state greenhouse effect"- Matson and Brown, 1989). Urquhart and Jakosky estimate that the depth of penetration on Europa is less than 2 cm and may cause a maximum subsurface temperature rise of 10 K.

The above data and analyses suggest that Europa's surface has a relatively low thermal inertia and cools rapidly to nighttime temperatures which may be a low as 80 K. The diurnal thermal skin depth is of the order of 7-8 cm (Urquhart and Jakosky, 1996). Subsurface temperatures, 10's of centimeters to 10's of meters below the surface, depending on the subsurface thermal gradient due to internal heat flow, are likely to be 100 K or lower over much of the surface.

1.6   Rheology

Water ice is a complicated material mechanically. At Europa's low surface temperatures it will behave as a strong solid, while at depth, as the temperature approaches the liquidus, it may have properties resembling terrestrial ice in glaciers, ice packs and sea ice.   This change in rheological behavior will affect the character of small and large-scale structures on the satellite's surface (Johnson and McGetchin, 1971). Small-scale geological features (small craters, scarps, etc.) should resemble similar features in strong, competent materials seen on rock planets and satellites, while large-scale features, which "sense" the warmer, less viscous layers below, may show the effects of viscous flow or relaxation. Voyager images revealed the absence of any major topographic features more than a few hundred meters in height and the absence of large, deep impact craters and basins. Both have been cited as evidence for a warm, soft ice layer below the cold, stiff surface ice crust (Passey and Shoemaker, 1982; Squyres and Croft, 1986). The mechanics of impact cratering is also affected by the properties of ice on satellites like Europa (see Chapman and McKinnon, 1986). Galileo data and analyses have greatly expanded the discussion of rheology and its relation to the observed landforms (Pappalardo *et al.*, 1998a,b). Note that all structural properties affected by gravity (such as stress due to surface loads) will scale to terrestrial examples by Europa's low gravity (~1/6 g).

The rheological properties of Europa's ice will also greatly affect the way heat (either radiogenic or tidal) is both generated and transported out of the interior and crust. One of the major uncertainties in calculations of the thermal history of Europa and whether a liquid layer can be sustained beneath the ice crust is the role played by solid state convection in the ice layer and how it responds to tidal forces (see Schubert *et al.*, 1986, Ojankangas and Stevenson, 1989; Squyres *et al.*, 1983).

1.7   Electromagnetic Properties

The electromagnetic properties of Europa's crust and interior are currently constrained by three data sets – radar observations of the satellite, Galileo measurements of magnetic fields and charged particles in Europa's vicinity, and existing laboratory and theoretical estimates of ice properties under Europa's conditions.

Radar observations of the icy satellites show they have unusual properties compared with "terrestrial" planets. The radar reflectance of these bodies is very high, and the nature of the echoes, in both their frequency and polarization characteristics, is completely unlike that seen for other planetary targets (Ostro 1982, 1990, 1992, 1993). Among the icy satellites, Europa stands out. It has the highest radar power albedo of any planetary body yet measured at 3.5 and 13 cm. These data have been interpreted as resulting from penetration of the radar waves meters or tens of meters into a low-loss, highly scattering medium. For all of these bodies, however, the radar albedo at 70 cm is much lower (Black *et al.*, 1996), in the case of Europa undetectable. This suggests a change in the volume scattering properties of the icy upper layer at approximately meter scales and larger.
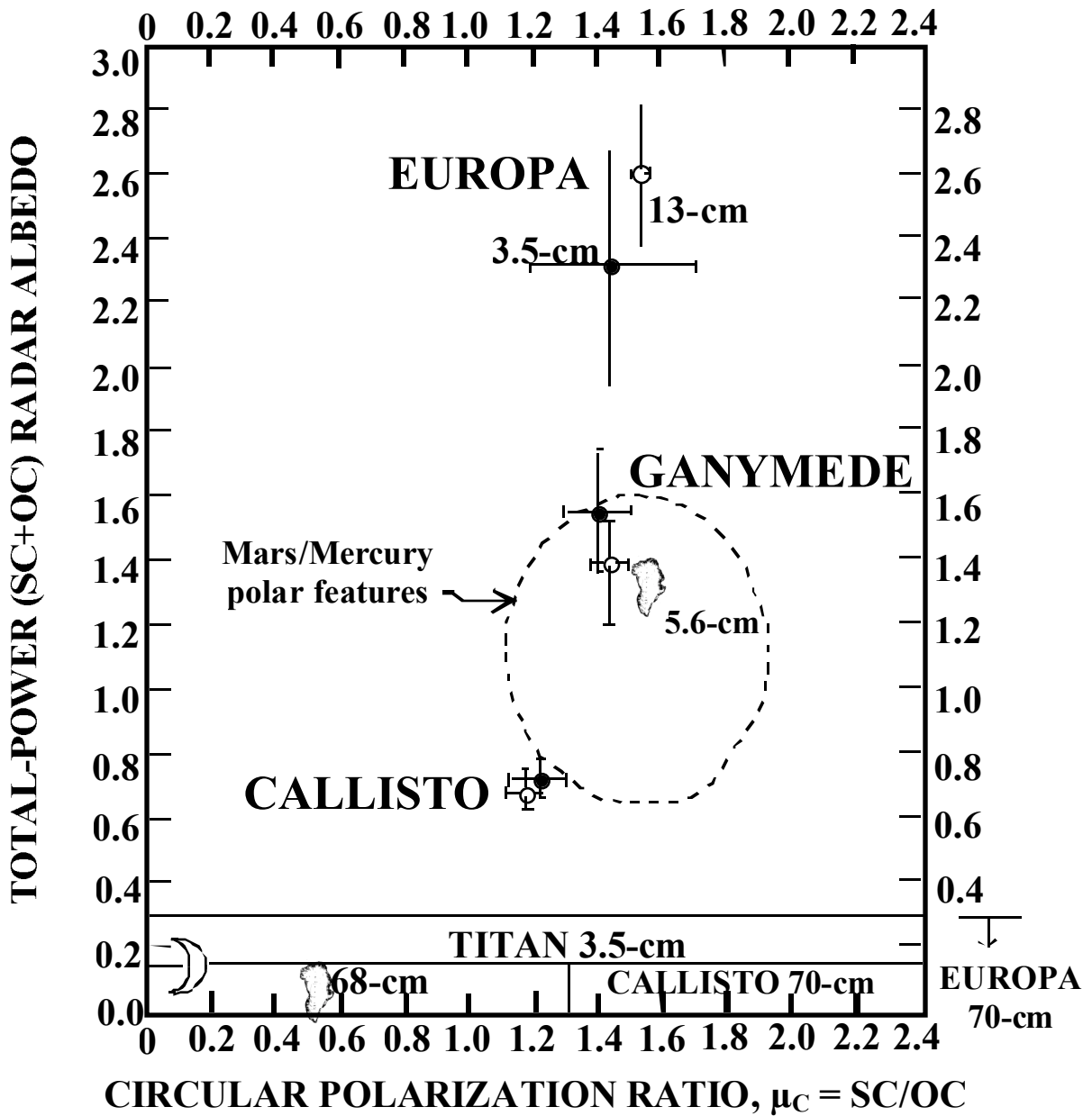
Figure 7.   Radar properties of Europa, Ganymede, and Callisto compared to those of some other targets. The icy Galilean satellites' total-power radar albedos do not depend on wavelength between 3.5 and 13 cm, but plummet at 70 cm. There are large uncertainties in those objects' μ_C at 3.5 cm (the only wavelength at which it has been detected by radar). Solid symbols shaped like Greenland indicate properties of that island's percolation zone at 5.6 and 68 cm. The domain of most of the bright polar features on Mars and Mercury is sketched.

Models for the electrical properties of ice and impurities at low temperatures have been constructed by Chyba *et al.* (1998) from existing laboratory and theoretical calculations. Combined with model temperature-depth profiles, these calculations place an upper limit of about 10 km on the likely depth to which long-wavelength (>~ 1 m) electromagnetic waves can penetrate Europa's surface. Major uncertainties exit in estimating the concentration, nature, and effects of impurities and the losses due to volume scattering of the type responsible for Europa's high radar albedo at 3.5 and 13 cm (see Sec. 2.1.3.3 of the Europa Orbiter Mission and Project Description document in the Outer Planets Program Library, which can be accessed over the Internet through URL http://outerplanets.LaRC.NASA.gov/outerplanets.). There are also uncertainties in the low temperature imaginary permittivity of ice in the frequency range of 10 – 100 Mhz (Chyba *et al.*, 1998; Lorenz, in press, 1998)

Europa's electrical properties also affect the way it interacts with the Jovian magnetospheric environment. A thin atmosphere, consisting at least of oxygen, has been detected along with an ionosphere (see next section). The absorption signature of high energy charged particles by Europa has been interpreted as due to a finite conductivity, possibly supplied by the ionosphere (Paranicas *et al.*, 1998).

During Galileo's close flybys of Europa, significant perturbations to the ambient Jovian magnetic field were observed by the Magnetometer experiment (MAG) (Khurana *et al*., 1998). Three types of interaction have been investigated by the authors: 1) currents produced by the pick-up of ions in a "cometary" type of interaction; 2) an intrinsic dipole field arising in the interior of Europa; and 3) an induced dipole moment arising from currents within a conducting shell produced by the time-varying Jovian field. The cometary interaction model is the preferred explanation for the strong perturbations seen on the twelfth orbit, when Europa was in the dense Jovian plasma near the magnetic equator. The signatures seen during the other orbits can be equally well fit by either an intrinsic field or the induced field model. The quality of fit by the induced field model is good, and by itself this is regarded as a significant point in its favor, since, given the assumption that Europa is acting as a conducting sphere, the magnitude and direction of the induced field are fixed, with no free parameters. Callisto also exhibits similar perturbation, and in this case, models for flybys at different magnetic latitudes provide a clear preference for the induced field model. A similar test has not yet been possible for Europa.
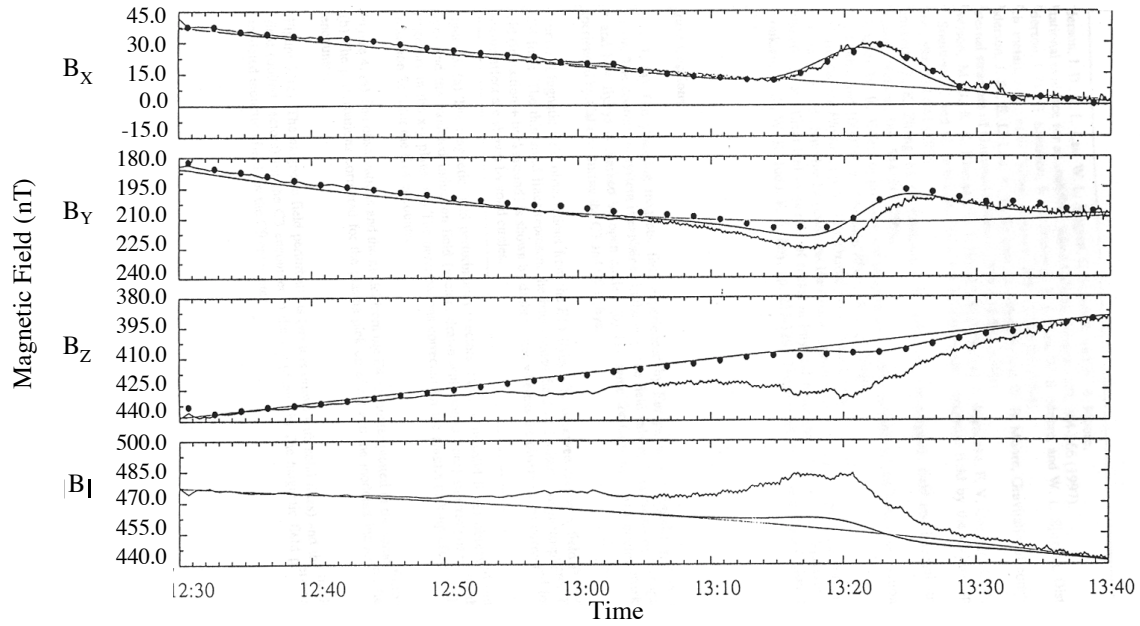
Figure 8.   Magnetic field observations from the E14 flyby. The observed magnetic field is shown by thick solid lines. The thin solid lines represent the background field of Jupiter's magnetosphere. The modeled field (induction + background) is shown by dashed lines whereas the observations corrected for the plasma pick-up effect are shown by solid circles.

If the induced field model is correct, it places important constraints on the conductivity of the upper portions of Europa's crust. In order to respond as a conducting shell, Europa's electrical conductivity must be high enough such that the skin depth calculated for a ten-hour periodic magnetic field variation (Jupiter's rotation period) is small with respect to the radius of the satellite. Plausible values for the conductivity of the ionosphere, ice, and rock are all orders of magnitude too small to satisfy this criterion. The conductivity of terrestrial seawater, however, is of the required order (~ 3 S/m) and yields a skin depth of 60 km. Khurana *et al.* conclude that a salty, conducting liquid ocean ~10 to 100 km thick would explain the magnetic signatures for both Europa and Callisto.

2.   **Magnetospheric Sputtering**

The interaction of charged particle radiation from Jupiter's magnetosphere with Europa's surface has been discussed in a number of contexts: 1) optical alteration of the surface, particularly in the ultraviolet, 2) erosion and redistribution of material on the surface and 3) production of a tenuous atmosphere (see reviews and references therein - Clark *et al.*, 1986; Cheng *et al.*, 1986; R. E. Johnson, 1998).

3.   Atmosphere

Data from ground and earth orbiting telescopes as well as Galileo data have contributed to our knowledge of Europa's extremely tenuous atmosphere. An *ad hoc* working group chaired by Dr. Donald M. Hunten of the University of Arizona was tasked with summarizing our current understanding of the atmosphere and assessing uncertainties. The following is their report to the Outer Planet Solar Probe project and the Europa Orbiter Science Definition Team.

This recommended model of Europa's atmosphere is based largely on an analysis by Saur (1998). That paper leans heavily on an HST observation of two UV lines of atomic oxygen by the HST (Hall, 1995, 1998) and is consistent with radio-occultation data from Galileo (Kliore, 1997). Ip (1998) presented an upper limit based on measurements of the flux of sputtering ions by the Energetic Particle Detector (EPD) on Galileo, generally consistent with the other results.

In 1977 Yung and McElroy proposed that an oxygen atmosphere would exist on Ganymede and by extension on other icy bodies like Europa. Water vapor should be present in some small quantity; photo dissociation should convert it slowly to H_2 and O_2 and the hydrogen should escape much more rapidly than the oxygen. These processes, as well as sputtering by the impact of positive ions, were adopted in the model given by Hall. Lanzerotti (1978) and Johnson (1982) had pointed out that sputtering is a much more likely source of molecules than evaporation, and this is the basis of the Saur model. Moreover, sputtering produces O_2 directly, as well as H_2O , so there is no need for the slow photolysis of the latter. UV emissions at 1304 (a triplet) and 1356 Å are excited by impact of magnetospheric electrons, which dissociate O_2 molecules and simultaneously excite one of the O atoms produced (Hall, 1995).

Table 1 shows a summary of available results for the day side. The composition is assumed to be essentially pure O_2 along with a small amount of water vapor to make up for the losses by its photolysis. There is excellent agreement between the abundance, or column density, obtained from the two analyses of the UV and the radio data. The amount of gas in the atmosphere is limited by the requirement that the ions which generate it by sputtering be able to reach the surface and is therefore unlikely to be significantly greater than the values quoted. The electron-density profiles obtained by Kliore (1997) give an estimate (quite uncertain) of the ionospheric scale height from which that of the neutral atmosphere follows directly. We suggest that the derived column abundance is also quite uncertain because the ionization rate by electron impact seems to be a factor of 8-10 too small. Saur (1998) found a similar scale height based on the measured oxygen line widths and the point-spread function of the GHRS aboard HST. The number density at the surface is simply the ratio of the column abundance to the scale height.

Table 1. Summary of Day Side Results

Authors		Abundance 10^{14} cm^{-2}	Scale Height km	Number Density 10^7 cm^{-3}
Hall	(1995)	15	---	---
Hall	(1998)	2-14	---	---
Kliore	(1997)	7.5	120	6
Saur	(1998)	5	145	3.5
Ip	(1998)	≤ 34	19	≤ 180

The paper by Ip (1998) uses the flux of sputtering ions measured by the Galileo EPD but then assumes an additional factor of 10 to account for secondary ions, presumably accelerated in a local electric field. A previous paper (Ip, 1996) assumed this factor to be only 1.2. The assumed scale height appears to use the surface temperature with no allowance for the heating found by Saur. The derived abundance, shown in Table 1 as an upper limit, is in reasonable agreement with the other papers. The large number density is directly traceable to the small assumed scale height; we therefore recommend the values given by Saur.

An atmosphere produced by sputtering would be expected to be denser on the upstream side than the downstream (relative to the Jovian plasma impacting the trailing hemisphere). Saur assumed that the variations of surface and column densities are directly proportional to the normalized sputtered fluxes calculated by Pospieszalka and Johnson (1989) and adopted a ratio of 2.3. However, the lifetime of O_2 is of order 2 Earth days, if the loss rate is as large as the 50 kg/sec given by these authors, and this should be long enough for a considerable redistribution.

Atomic oxygen will be present in some small abundance. A simple mass-balance calculation, equating the production and loss of O, gives a mixing ratio O/ O_2 of 0.01. An upper limit is obtained from Hall (1995) who finds the best fit to the HST data with no O at all with an upper limit of about 0.1. Effects on spacecraft surfaces should be much less than for many Earth-orbiting spacecraft, which fly in much larger densities of essentially pure atomic oxygen and at much higher velocities.

Another important variable is temperature; if the night side were significantly cooler than the day side, gas would be concentrated on the cool night side and the density at the surface could vary by as much as the -5/2 power of the temperature (e.g. Chamberlain and Hunten 1987). The variation is smaller at high altitudes because the scale height is smaller at a lower temperature. However, it is unlikely that the temperature varies significantly around the body because it is probably controlled by the large ejection velocities of sputtered atoms.

We conclude that density variations are unlikely to exceed a factor of around 2 as a function of either solar zenith angle or angle relative to the impacting plasma.

W. Sjogren has investigated the possibility that atmospheric drag may have been detected on one of Galileo's close passes. He has informed us that ". . . the investigation is very marginal and we think that the small signal in the data is more than likely a plasma effect on the S-band". Perhaps there will be a better opportunity during the Galileo Europa Mission.

SUMMARY

1. For day side density, abundance or integrated density, and scale height we recommend the Saur values in the second-last line of Table 1.

2. The ratio of O to O_2 number densities is about 0.01 with an upper limit of 0.1.

3. The ratio of abundance's on the downstream and upstream (or day and night) sides is unlikely to exceed a factor of 2.

REFERENCES

Chamberlain, J. W. and D. M. Hunten 1987. *Theory of Planetary Atmospheres* (Academic Press), pp. 361-365.

Hall, D. T., D. F. Strobel, P. D. Feldman, M. A. McGrath and H. A. Weaver 1995. Detection of an oxygen atmosphere on Jupiter's moon Europa, *Nature* 373, 677-679.

Hall, D. T., P. D. Feldman, M. A. McGrath and D. F. Strobel 1998. The far-ultraviolet oxygen airflow of Europa and Ganymede, *Astrophys. J.*, in press for May 1998.

Ip, W. H. 1996. Europa's oxygen exosphere and its magnetospheric interaction, *Icarus* 120, 317-325.

Ip, W. H., D. J. Williams, R. W. McEntire and B. H. Mauk 1998. Ion sputtering and surface erosion at Europa, *Geophys. Res. Lett.* 25, 829-832.

Johnson, R. E., L. J. Lanzerotti and W. L. Brown 1982. Planetary applications of ion induced erosion of condensed-gas frosts, *Nucl. Insts. and Methods* 198, 147-157.

Kliore, A. J., D. P. Hinson, F. M. Flasar, A. F. Nagy and T. E. Cravens 1997. The ionosphere of Europa from Galileo radio occultations, *Science* 277, 355-358.

Lanzerotti, L. J., W. L. Brown, J. M. Poate and W. M. Augustyniak 1978. On the contribution of water products from Galilean satellites to the Jovian magnetosphere, *Geophys. Res. Lett.* 5, 155-158.

Pospieszalska, M. K. and R. E. Johnson 1989. Magnetospheric ion bombardment profiles of satellites Europa and Dione, *Icarus* 78, 1-13.

Saur, J., D. F. Strobel and F. M. Neubauer 1998. Interaction of the Jovian magnetosphere with Europa: Constraints on the neutral atmosphere, *J. Geophys. Res.*, 103, 19,947-19,962, 1998.

April 17, 1998

4. Geology

The Voyager mission in 1979 provided the first close-up look at Europa's surface. Although limited to relatively low surface resolution (~ 4 km at best), Voyager's images revealed a satellite remarkably different from any of its neighbors. Summaries of the geology and tectonics of Europa based on Voyager data can be found in Lucchitta and Soderblom (1982), Malin and Pieri (1986), and Squyres and Croft (1986). They describe a geologically young planetary surface, with only a few recognizable impact craters. Long "linea" crisscross-cross the surface in what appears to be a global pattern of fractures. The bulk of the surface is divided between bright plains units and somewhat darker "mottled terrain", with the trailing

18

hemisphere having the greater proportion of the mottled unit. Near-terminator images show a fine mesh of low ridges, but both terminator and limb images show no topography exceeding a few hundred meters in height anywhere on the satellite.   These general features can all be recognized in global views of Europa from Galileo.
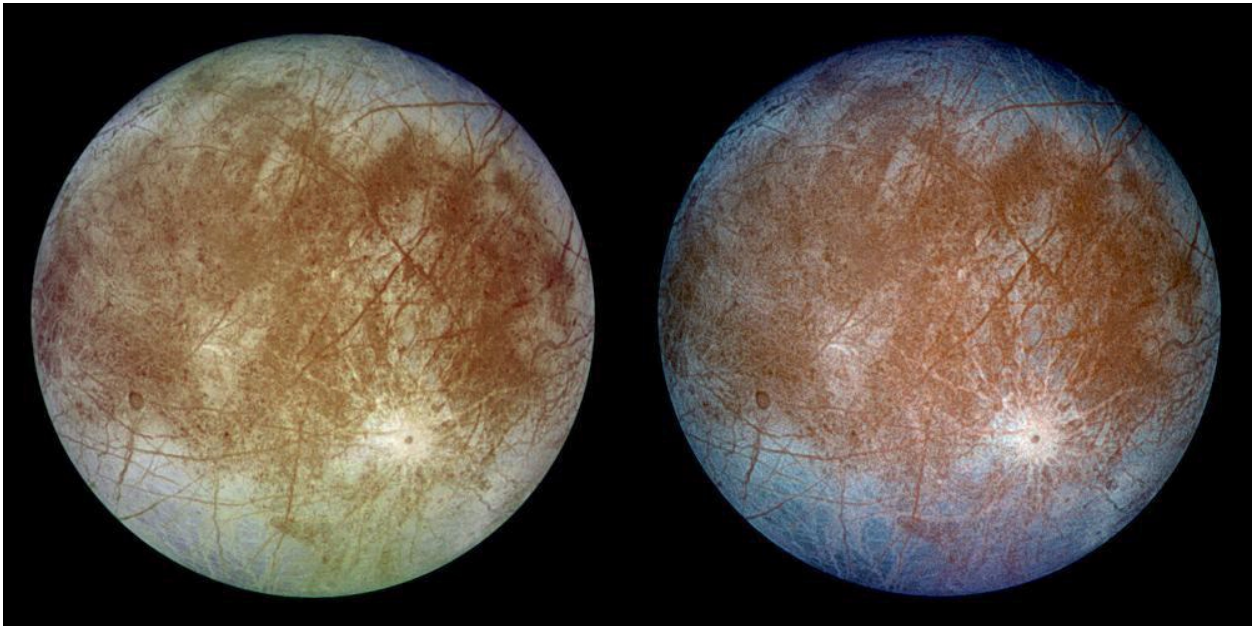

Figure 9.   Global view of Europa (natural and false color) from *Galileo*.

Data from Galileo have tremendously increased our knowledge of Europa's geology. Much of the data is still being analyzed and for details, the reader should refer to the most recent publications (Belton *et al.*, 1996; *Nature*, 391, 22 January 1998; *Icarus* special issue, 1998). Key findings bearing on the prime objectives of the Europa Orbiter mission are briefly summarized below.

4.1   Structures/Topography

In Galileo images, ranging in resolution from ~10 m to 100's of meters, the major structures seen dimly in Voyager's pictures come into sharp focus. The linea are seen to be long, very regular ridge systems, a few hundred meters in height and a few kilometers wide. Most have a medial trough or valley, typically a few hundred meters wide. The youngest ridges stratigraphically are the highest and usually consist of a bright ridge flanked on both sides by a regular pattern of darker material, sometimes diffuse in appearance. When seen at lower resolution, this produces the effect referred to in the Voyager literature as a "triple band" (a dark-bright-dark brightness pattern across the linea). These prominent linea literally span Europa's globe, stretching for hundreds to thousands of kilometers with little change in their basic morphology and are obviously associated with large scale crustal stress patterns. More complex ridge systems, with multiple parallel ridges, troughs and fractures, are also seen.

Some ridge systems, most concentrated in the "pull apart" terrain near the anti-Jupiter point on the surface, form wedge-like structures with a high degree of axial symmetry, resembling in some respects sea-floor spreading centers on the Earth.
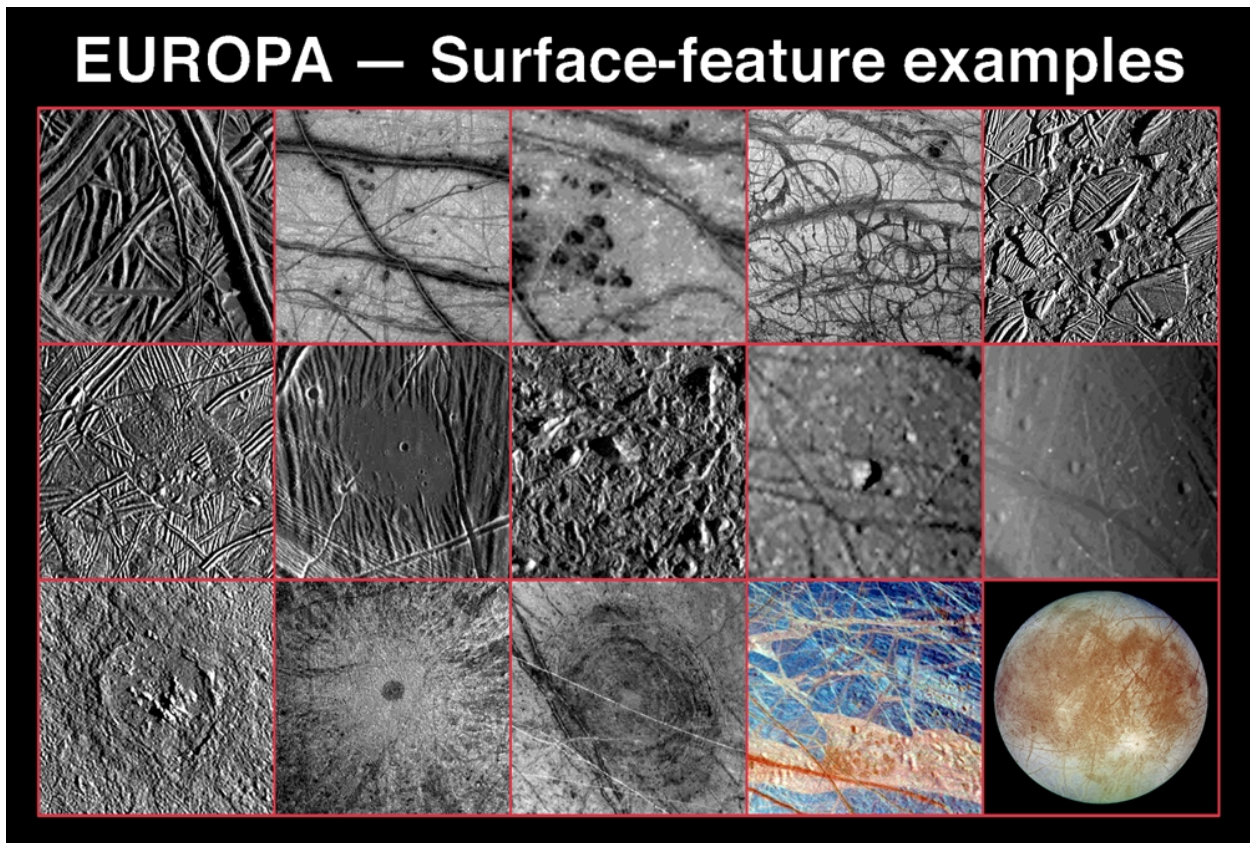

Figure 10.   Image available from http://photojournal.jpl.nasa.gov/newarchive/PIA00746.tiff

The bright plains units, when examined at high resolution, display a complex pattern of intersecting ridges and ridge systems of all apparent ages, predominantly brighter and of lower relief than the global scale linea. The geological relationships between the ridges in the plains units include ubiquitous examples of strike-slip offsets, implying a complex history of ridge formation and displacement. The bright plains have been modified in three basic ways: by formation of new crust in the wedge regions; by destruction of plains crust in the mottled terrains; and by relatively sparse medium-scale impact scars that disrupt the plains in places.

In the wedge regions, older ridged plains have been separated by the formation of the wedges, and the pieces displaced from one another as coherent plates. Computer modeling demonstrates that, with the wedge units removed, these regions can be fit back together, much like a gigantic jigsaw puzzle, implying that pre-existing plains units were not destroyed in the process. The stratigraphic relationships among the various younger linea crossing these areas

can also be reconstructed in this way, by noting which structures are "re-joined" to one another when the wedges are geometrically removed.

The mottled terrain and the various darker patches and spots seen in Voyager and Galileo low-resolution images apparently are among the youngest regions on Europa and are areas of large scale destruction of ridged plains crust. The nature of the crustal destruction in these regions has been interpreted as implying thermal activity in Europa's crust at relatively shallow depths (<~10 km). This, together with the general geologic youthfulness of the surface as a whole, is one of the strongest arguments for the existence of a global liquid ocean layer recently in Europa's history. These regions are now known as "chaos". The smaller spots, called "lenticulae" (a Voyager era nomenclature) seem in high-resolution Galileo pictures to be mostly small patches of "chaos".

The best studied of the chaos regions to date is Conamara Chaos located at about 13 N, 273 W. In this large region, bounded by two prominent linea, many large blocks of ridged plains have been broken off from the borders of the region, and the interior consists of a lower lying chaotic matrix with many blocks of ridged plains scattered about, separated from one another. Many of the blocks appear to be rotated from their original orientations, and some are tilted from the horizontal as well. Here again the jigsaw puzzle analogy applies, but in this case many of the pieces have gone missing. Computer reconstruction of this region suggests that about half of the pre-existing crust is no longer there - melted, sunk or otherwise disposed of.

Impact cratering has affected the surface of Europa, but to a far lesser extent than on Ganymede and Callisto. There are no recognizable impact structures larger than about 20-50 km (estimated size of the original "transient" crater). Even 20-km sized impacts, ubiquitous on the other icy satellites, are rare. There appear to be less than about a dozen structures in this size range, and they all show varying degrees of the morphological signatures suggesting impact into a low-viscosity medium. Some impact scars, such as Tyre Macula, show no visible crater depression at all, being a large structure of concentric fractures surrounded by swarms of secondary impact craters. Pwyll, probably the youngest large impact crater on the satellite, has a more "normal" crater morphology with an extensive ray system, ejecta deposits, a raised rim and a central peak, but its floor is level with the surrounding terrain, suggesting viscous rebound during or after crater formation. Smaller craters are evident in many images and appear similar to small fresh craters on many planetary surfaces, consistent with being formed in the thin, cold, high-viscosity upper crust. Many of the small craters are thought to be secondary impacts formed by ejected material from larger craters such as Pwyll.

4.2   Crater statistics/surface age

The absolute age of the features seen on Europa's surface is obviously of great interest in assessing the geological history of the satellite and the likelihood that a subsurface ocean exists at the current epoch. Unfortunately, although crater statistics provide good evidence for the relative age of planetary surfaces, deriving an absolute age from crater statistics alone is extremely difficult and fraught with many uncertainties. The major source of uncertainty and

debate over the age of surfaces in the Jupiter system is the wide range of estimates of the flux of impacting bodies through the system during the last 3-4 billion years. Shoemaker and Wolfe (1982) based their estimates on dynamical calculations showing that extinct Jupiter-family comets should be the primary source of impactors in the system and extrapolations from the (small) number of known objects in this class to derive the total population. Their calculations result in a relatively young age for Europa's surface, less than ~100 myr. Later revisions of the comet population estimate as more were discovered led Shoemaker (1996) to suggest even younger ages, < ~ 1 myr for much of the surface.

Other estimates, based on the relative cratering among the icy satellites and a belief that the youngest basins on Ganymede should date to the end of "heavy bombardment", 3.8 byr, result in much older ages – 0.5 – 3.0 byr (Neukum, 1997,1998). Zahnle *et al.* (1998) has recently addressed this problem by making an assessment of the celestial mechanics associated with the delivery of bodies from the Kuiper belt to cometary orbits (Levison and Duncan, 1997). This study is also supported by the statistics of the number of comets that have come close enough to Jupiter to be captured in historic times, Shoemaker-Levy 9 being the most spectacular example. Their conclusions support the younger ages advocated by Shoemaker but with an estimated uncertainty of about a factor of five. In summary, the weight of opinion currently suggests that much of the present surface of Europa is no more than 50-100 million years old.

4.3   Tectonics

The global lineament system on Europa is assumed by most researchers to be a fracturing response to a global stress pattern. An obvious candidate for producing these patterns is tidal stress. Several studies of the Voyager lineament orientations concluded that tidal despinning would not produce the observed patterns but that other combinations of orbital change and eccentricity might work (Helfenstein and Parmentier, 1983). The possibility of a global liquid ocean also raised the theoretical issue of non-synchronous rotation of a decoupled icy shell over a silicate interior (Greenberg and Weidenshcilling, 1984). The stress patterns predicted for this situation are more consistent with the Voyager lineament orientations (Helfenstein and Parmentier, 1985; McEwen, 1986). Galileo's data allow the history of some of the lineaments to determined from color and stratigraphic relations. These data support the proposed non-synchronous rotation model, but do not determine the time-scale. However, the lack of measurable change in surface feature position in the twenty years between Voyager and Galileo place an lower limit on the period of rotation with respect to Jupiter of 10^4 yrs (Greenberg *et al.*, 1998a).

Tectonic forces are probably involved both in the construction of the ridge systems and in the destruction of plains units in the chaos regions. There are currently several models for ridge formation, most involving initiation by movement along fractures in the ice crust and infilling by new material from below (e.g. Sullivan *et al.*, 1998; Greenberg *et al.*, 1998b; Head *et al.*, 1998). Solid state convection in the form of diapirism has also been invoked to explain

aspects of both the ridges and the "pits, spots and domes" that are also related to chaos type activity (Pappalardo *et al.*, 1998a,b)

5.   Surface Composition

As noted in the earlier discussion of spectral albedo, water ice/frost is a major constituent of the surface of Europa. The optical data technically pertains only to the top surface (0.1 to ~ 1 mm depending on optical properties). The gravity data, which require a substantial crust of low density (~1 gm/cm^3) material, strongly suggest that the upper 100 km or so is dominated by water in some form. Most of the compositional discussion concerning Europa has thus centered on identifying any non-water ice materials on the surface and trying to determine their origin, exogenic or endogenic. In a bright, transparent material like ice, even very small amounts of contaminant material can have a great effect on the spectrum (e.g. Clark, 1981). Based on laboratory studies of these effects, it has been estimated that on average Europa's surface contains no more than a few weight percent of non-ice material (Sill and Clark, 1982; Clark *et al.*, 1986). Also, as mentioned earlier, exogenic modification by plasma bombardment of the surface has been suggested as an explanation for the ultraviolet spectral characteristics.

A review of pre-Galileo information about Europa spectra and compositional interpretations can be found in Calvin *et al.* (1995).   They note once again that the hemispheric telescopic spectra are dominated by water ice absorption features in the near infrared, but modified by some ultraviolet absorbing contaminant at short wavelengths. The leading hemisphere spectrum is fit reasonably well by frost spectra with grain sizes in the 100-µm range. A remaining puzzle in interpreting the ground-based spectra is the peculiar nature of the trailing hemisphere spectrum. While similar in general characteristics to the leading hemisphere spectrum, the trailing spectrum shows some significant differences. In particular, the 1.5- and 2.0-µm absorption features are notably distorted and asymmetric compared with those on the leading hemisphere and spectra of laboratory frosts. Clark (1980) discussed these features and suggested that long optical paths through "block ice" with only a thin coating of frost could explain some of the features of the trailing spectrum. He noted however that the 2.0-µm absorption in the trailing hemisphere spectrum remained more asymmetric than any ice or frost spectra and suggested that mixtures with small amounts of other minerals might be required to explain the differences.

Galileo spectral data have shed new light on the problem of identifying the non-water ice components in the surface by identifying the geologic locations where they occur in the greatest concentrations. Mulitspectral images show that young linea and chaos regions (the "mottled terrain") have the strongest visible and near-infrared coloration, due presumably to non-water ice contamination (Geissler *et al.*, 1998). Near Infrared Mapping Spectrometer spectra of these areas display the distorted absorption features seen in the trailing hemisphere spectra. In these areas the distortion is even more marked, since the hemispheric spectra represent a mix of spectral information from these regions along with areas dominated by more normal ice spectral characteristics (McCord *et al.*, 1998a).   The spectral differences between

the hemispheres appear to be due primarily to the larger area covered by these units on the trailing hemisphere.

The compositional identification of the non-water ice constituent is still a matter of debate and on-going research. McCord *et al.* (1998a) have suggested that heavily hydrated salt minerals (Na, Mg, sulfates and carbonates with five to seven water units attached) are the best candidates for explaining the highly distorted spectral characteristics. Dalton and Clark (1998) argue based on terrestrial analog spectra that long optical paths in glaze or bubbly ice are a better explanation (similar to Clark's 1980 discussion of the trailing hemisphere spectrum). McCord *et al.* (1998b) have countered some of these arguments and continue to contend that mixtures of hydrated salts are the best candidates. In either case, McCord *et al.* (1998a,b) have demonstrated that spectra of regions with the strongest distorted absorption "signature" are very similar wherever they occur on Europa's surface, suggesting a global process and/or uniform composition.

Salts of one form or another are, of course, not an unreasonable material to expect if Europa has or has had extensive liquid water activity. For instance, magnesium sulfate and other salts are found in aqueously altered meteorites. Evaporite salt deposits on Io were suggested before the massive level of volcanic activity was discovered (Fanale *et al.*, 1977), and the same geochemical arguments could easily apply to Europa's evolution (Squyres and Croft, 1986; Kargel, 1991). Fanale and colleague have recently performed more extensive laboratory studies of meteorite leach systems and studied the resulting brines (Fanale *et al.*, 1998).

6.   Ice Crustal Models

For the purposes of comparing various experimental approaches to addressing Europa Orbiter objectives, the Radar Instrument Definition Team (see report) suggested three simplified models for the distribution of ice and water on Europa. Investigators should consider that any of these cases (or variants thereof) might in principle describe Europa globally or occur in some regions. These are provided only to stimulate thought about possible outcomes.

1.   Thick convecting ice over rock

If Europa does not have a global liquid water ocean, either because it never formed or because it has subsequently frozen, the expected structure of the crust is:

- A thin, cold conductive layer possibly kilometers thick. T~100 K at the surface with the temperature rising with depth down to -
- A thick, warm convecting layer near the liquidus (isothermal with T~250 K depending on contaminants etc.) up to 100-130 km thick extending down to the rock interface (with unknown topography, but probably not exceeding a few kilometers)

A possible variant might possess a very thin (~ kilometers ?) unfrozen briny liquid layer between the underlying rock and the convecting ice.

2. Thin conducting ice over liquid

If there are regions on Europa where liquid water has come close to or to the surface recently or if tidal heating of the crust has frustrated cooling by convection globally the structure could be:

- Thin, cold conducting ice as in 1.) – meters (?) to kilometers thick
- Water at ~270 K , ~100 kilometers deep

3. Thick ice layer over water

If solid-state convection does play a role in crustal processes but is not sufficient to completely freeze the ocean, the structure might resemble a mixture of 1.) and 2.):

- Thin cold conducting ice kilometers thick
- Thin warm convecting ice 10 – 20 kilometers thick, isothermal to –
- Water at ~270 K, ~100 kilometers deep

Some members of the SDT feel that 3.) may be the best global description of Europa at the current time based on the various observations and models discussed in the bulk of this section (see also Pappalardo *et al.*, 1998b).

Table 6:   Summary of estimates of Europa ice shell thickness (from Pappalardo, et al., 1998b)

Ice Shell Portion	Thickness (km)	Estimation Technique	Reference
effective elastic lithosphere	0.4	ridge-induced flexure	*Tufts et al., 1997*
effective elastic lithosphere	0.1 - 0.5	dome-induced flexure	*Williams and Greeley, 1998*
elastic lithosphere	~1 - 2	flexure correction factor	*Pappalardo et al., 1998b*
tensile lithosphere	≤ 1	fracture mechanics	*Moore et al., 1998*
local rigid portion of shell	≤ 3	dimension of chaos plates	*Carr et al., 1998*
local shell thickness	2	buoyant blocks	*Carr et al., 1998*
local shell thickness	0.2 - 3	buoyant blocks	*Williams and Greeley, 1998*
convective sublayer	≥ 2 -8	initiation of convection	*Pappalardo et al., 1998a*
convective sublayer	< 40	diapir rise time	*Rathbun et al., 1998a, 1998b*
whole ice shell	> 12	initiation of convection	*McKinnon, submitted*
whole ice shell	6 - 15	large impact morphologies	*Turtle et al., 1998*

7.   References:

1. Anderson *et al.*, *Nature*, 384, 541, 1996

2. Anderson *et al.*, *Science*, 281, 2019-2022,1998

3. Belton *et al.*, *Science*, 274, 377-385, 1996

4. Belton *et al.*, *Nature*, 391, 22 January 1998

5. Belton, *et al., Icarus* special issue, vol. 135, #1, 1998

6. Black *et al.*, The icy Galilean satellites: 70cm wavelength radar properties, *Lunar Planet Sci.Conf*. 27th, 121, 1996

7. Buratti, B. and J. Veverka, "Voyager Photometry of Europa", *Icarus*, Vol 55, Iss 1, pp 93-110, 1983

8. Buratti and Golombek, *Icarus*, 61, 208-217, 1985

9. Calvin *et al.*, *J. Geophys. Res.*, 100, 19,041-19,048, 1995

10. Carr, M. H., M. J. S. Belton, C. R. Chapman, M. E. Davies, P. Geissler, R. Greenberg, A. S. McEwen, R. Greeley, R. Sullivan, J. W. Head, R. T. Pappalardo, K. P. Klaasen, T. V. Johnson, J. Moore, G. Neukum, G. Schubert, J. A. Burns, P. Thomas, and J. Veverka, Evidence for a subsurface ocean on Europa, *Nature, 391*, 363-365, 1998.

11. Cassen *et al.*, Geophys. Res. Lett., 6, 731-734, 1979

12. Cassen *et al.*, Geophys. Res. Lett., 7, 987-988, 1980

13. Cassen *et al.*, *Satellites of Jupiter* (ed. D. Morrison, U. of Arizona Press, Tucson), 93-128, 1982

14. Chapman and McKinnon, *Satellites* (eds. J. A. Burns and M. S. Matthews, U. of Arizona Press, Tucson), 492-580,1986

15. Cheng *et al.*, *Satellites* (eds. J. A. Burns and M. S. Matthews, U. of Arizona Press, Tucson), 403-436,1986

16. Chyba et al., *Icarus*, 134, 292-302, 1998

17. Clark, *Icarus*, 44, 388-409,1980

18. Clark, *J. Geophys. Res.*, 86, 3074-3086, 1981

19. Clark *et al.*, *Satellites* (eds. J. A. Burns and M. S. Matthews, U. of Arizona Press, Tucson), 437-491,1986

20. Clark, *et al., Icarus*, 135, 95-106, 1998

21. Dalton and Clark, *BAAS*, DPS abstract, 1998

22. Fanale *et al.*, *Planetary Satellites* (J. A. Burns, ed., U. of Arizona Press, Tucson), 379-405, 1977

23. Fanale *et al.*, *Lunar Plant. Sci. Conf. XXIX*, abstract #1248 (CDROM), 1998

24. Geissler *et al.*, *Icarus*, 135, 107-126, 1998

25. Greenberg and Weidenshcilling, *Icarus*, 58, 186-196, 1984

26. Greenberg *et al.*, *Nature*, 391,368-370, 1998a

27. Greenberg *et al.*, *Icarus*, 135, 64-78, 1998b

28. Hansen, *Icarus*, 18, 237-246 1973

29. Head *et al.*, *Lunar Planet. Sci. Conf., XXIX*, abstract #1414 (CROM), 1998

30. Helfenstein and Parmentier, *Icarus*, 53, 415-430, 1983

31. Helfenstein and Parmentier, *Icarus*, 61, 175-185,1985

32. Helfenstein, *et al., Icarus*, 135, 41-63, 1998

33. Johnson, R. E., *Solar System Ices* (eds. Schmitt, De Bergh, and Festou, Kluwer, Dordrecht/Boston/London), 303-336, 1998

34. Johnson, T. V. and McGetchin, *Icarus*, 18, 612-620,1971

35. Johnson, T. V. *et al.*, *J. Geophys. Res.*, 88, 5789-5805, 1983

36. Kargel, *Icarus*, 94, 368-390, 1991

37. Khurana *et al.*, *Nature*, in press, 1998

38. Kuiper, *Astron. J.*, 62, 295(abstract), 1957

39. Levison and Duncan, *Icarus*, *117*, 13-32, 1997

40. Lorenz, in press, 1998

41. Lucchitta and Soderblom, *Satellites of Jupiter* (ed. D. Morrison, U. of Arizona Press, Tucson), 521-555, 1982

42. Malin and Pieri, *Satellites*, (eds. J. A. Burns and M. S. Matthews, U. of Arizona Press, Tucson), 689-717,1986

43. Matson and Brown, *Icarus*, 77, 67-81,1989

44. McCord *et al.*, *Science*, 280,1242-1245 1998a

45. McCord *et al. J. Geophys. Res.*, in press, 1998b

46. McEwen, *Nature*, 321, 49-51, 1986

47. McKinnon, W. B., Convective instability in Europa's floating ice shell, *Geophys. Res. Lett.*, submitted.

48. Millis and Thompson, *Icarus*, 26, pp.408-419,

49. Moore, J. M., E. Asphaug, R. J. Sullivan, J. E. Klemeszewski, K. C. Bender, R. Greeley, P. E. Geissler, A. S. McEwen, E. P. Turtle, C. B. Phillips, B. R. Tufts, J. W. Head III, R. T. Pappalardo, K. B. Jones, C. R. Chapman, M. J. S. Belton, R. L. Kirk, and D. Morrison, Large impact features on Europa: Results of the Galileo nominal mission, *Icarus, 135*, 127-145, 1998

50. Moroz, *Astron. Z.*, 42, 1287-1295, trans. *Soviet. Astron A. J.*, 9, 999-1006, 1965

51. Morrison, *Planetary Satellites* (ed. J. A. Burns, U. of Arizona Press, Tucson), 269-301, 1977

52. Neukum, *The Three Galileo's: The Man, the Spacecraft, the Telescope* (C. Barbieri et al,. eds.), Kluwer Academic, The Netherlands, 201-212, 1997

53. Neukum *et al.*, *Lunar Planet . Sci. Conf., XXIX* abstract #1742 (CDROM), 1998

54. Ojkangas and Stevenson, *Icarus*, 81, 220-241, 1989

55. Orton *et al.*, *Science*, 274, 369-391, 1996

56. Ostro, S.J., Radar properties of Europa, Ganymede, and Callisto. *Satellites of Jupiter* (ed. D. Morrison, U. of Arizona Press, Tucson), 213–236, 1982.

57. Ostro, S.J., and E.M. Shoemaker 1990. *Icarus*, 85, 335–345, 1990

58. Ostro, S.J., *et al.*, *J.Geophys.Res*. 97, 18,227–18,244, 1992

59. Ostro, S.J., *Rev. of Modern Physics*, 65, 1235-1279, 1993

60. Pappalardo, R. T., J. W. Head, R. Greeley, R. J. Sullivan, C. Pilcher, G. Schubert, W. Moore, M. H. Carr, J. M. Moore, M. J. S. Belton, and D. L. Goldsby, Geological evidence for solid-state convection in Europa's ice shell, *Nature, 391*, 365-368, 1998a

61. Pappalardo *et al.*, *J. Geophys. Res.*, submitted, 1998b

62. Paranicas *et al.*, *J. Geophys. Res.*, 103, 15,001-15,007, 1998

63. Passey and Shoemaker, *Satellites of Jupiter* (ed. D. Morrison, U. of Arizona Press, Tucson), 379-434, 1982

64. Peale *et al.*, *Science*, 203, 892-894, 1979

65. Pilcher *et al.*, *Science*, 178,1087-1089, 1972

66. Rathbun, J. A., G. S. Musser, Jr., and S. W. Squyres, Ice diapirs on Europa: Implications for liquid water, *Geophys. Res. Lett.*, submitted. 1998a

67. Rathbun, J. A., G. S. Musser, Jr., and S. W. Squyres, Thermal-mechanical properties of possible ice diapirs on Europa, *Lunar Planet. Sci. Conf., XXIX*, abstract #1087 (CD ROM), 1998b

68. Schubert *et al.*, *Satellites* (eds. J. A. Burns and M. S. Matthews, U. of Arizona Press, Tucson), 224-292, 1986

69. Shoemaker and Wolfe , *Satellites of Jupiter* (ed. D. Morrison, U. of Arizona Press, Tucson), 277-339, 1982

70. Shoemaker, *Europa Ocean Science Conference*, Capistrano Conference No. 5, San Juan Capistrano Research Institute, San Juan Capistrano, CA, 65-66,1996

71. Showman *et al.*, *Icarus*, 129, 367-383, 1997

72. Sill and Clark, *Satellites of Jupiter* (ed. D. Morrison, U. of Arizona Press, Tucson), 174-212,1982

73. Spencer (1987, U. of Arizona thesis)

74. Squyres *et al.*, *Nature*, 301, 225-226, 1983

75. Squyres and Croft, *Satellites* (eds. J. A. Burns and M. S. Matthews, U. of Arizona Press, Tucson), 293-341, 1986

76. Sullivan *et al.*, *Nature*, 391, 371-372, 1998

77. Tufts, B. R., R. Greenberg, P. Geissler, G. Hoppa, R. Pappalardo, and the Galileo Imaging Team, Crustal displacement features on Europa, *GSA Abstr. with Prog., 29*, A-312, 1997.

78. Turtle, E. P., C. B. Phillips, A. S. McEwen, J. M. Moore, R. Greeley, and the Galileo SSI Team, Numerical Modeling of Multi-Ring Impact Craters on Europa: Implications for Subsurface Structure, *Lunar Planet. Sci, Conf. XXIX*, abstract #1325, Lunar and Planetary Institute, Houston (CD ROM), 1998.

79. Urquhart and Jakosky, *J. Geophys. Res.*, 101, 21,169—21,176, 1996

80. Williams, K. K. and R. Greeley, Estimates of ice thickness in the Conamara Chaos region of Europa, *Geophys. Res. Lett.*, submitted.

81. Yoder, C.F., "Astrometric and Geodetic Properties of Earth and the Solar System," Global Earth Physics: A Handbook Of Physical Constants, p.19, 1995

82. Zahnle *et al.*, *Icarus*, in press, 1998